ELSEVIER

Catalysis Today 69 (2001) 399–408

CATALYSIS TODAY

www.elsevier.com/locate/cattod

Structured reactors for kinetic measurements under severe conditions in catalytic combustion over palladium supported systems

G. Groppi*, W. Ibashi[1], E. Tronconi, P. Forzatti

Dipartimento di Chimica Industriale e Ingegneria Chimica "G. Natta", Politecnico di Milano, Piazza Leonardo da Vinci 32, 20133 Milan, Italy

Abstract

The collection of chemical kinetics data in catalytic combustion over very active palladium catalysts under conditions relevant to practical applications (e.g. gas turbine combustors) is extremely difficult, mainly due to strong exothermicity and very fast rate of combustion reactions. Within this purpose in this paper two types of laboratory structured reactors, which closely resemble industrial monolith catalysts, are investigated: (a) the annular reactor, consisting of a catalyst coated ceramic tube, co-axially placed in a quartz tube; (b) the metallic plate-type reactor, consisting of an assembled packet of metallic slabs coated with a ceramic catalytic layer.

The design of the annular reactor configurations for kinetic investigations is first addressed by mathematical modeling. The resulting advantages, including: (i) negligible pressure drops; (ii) minimal impact of diffusional limitations in high temperature–high GHSV experiments; (iii) effective dissipation of reaction heat are then experimentally demonstrated for the case of CH_4 combustion over a PdO/γ-Al_2O_3 catalyst with high noble metal loading (10% (w/w) of Pd).

The feasibility of a near-isothermal operation with the metallic plate-type reactor by an extremely effective dissipation of reaction heat through proper selection of highly conductive support material and of the geometry of the metallic slabs is finally discussed and experimentally demonstrated for the case of combustion of CO at high concentrations over a PdO/γ-Al_2O_3 (3% (w/w) of Pd) catalyst.

Keywords: Structured catalyst; Kinetic measurements; Catalytic combustion; Palladium

1. Introduction

Catalytic combustion, which has been commercially applied for a long time to the elimination of organic compounds in the tail stream of combustion and industrial processes, is now coming into the market as a method for the production of heat and energy with minimal environmental impact [1]. After a successful demonstration project of more than 7400 operation hours with NO_x emissions below 2 ppm (at 15% O_2) and CO and unburned hydrocarbons emissions below 2 and 1 ppm, respectively, Catalytica has announced that three 1.5 MW Kawasaki M1A13X gas turbine generator packages equipped with the XONON catalytic combustion technology are currently expected to enter service in late 2001 for a Massachusetts healthcare facility of a US government agency [2]. Also domestic

* Corresponding author. Tel.: +39-02-2399-3258; fax: +39-02-7063-8173.
E-mail address: gianpiero.groppi@polimi.it (G. Groppi).
[1] On leave from Environmental Process Development Department, Industrial Machine and Plant Development Center, Ishikawajima-Harima Heavy Industries Co., Ltd., Yokohama, Japan.

0920-5861/01/$ – see front matter
PII: S0920-5861(01)00398-4

Nomenclature

C_f	concentration (mol/m^3)
$d_h = 2[r_0 - (r_i + \delta_w)]$	hydraulic diameter (m)
$D_{e,f}$	intraporous diffusivity (m^2/s)
$D_{ea,f}$	effective axial diffusivity (m^2/s)
$D_{m,f}$	molecular diffusivity (m^2/s)
$K_{g,f}$	mass transfer coefficient (m/s)
L	catalyst length (m)
n	catalyst coordinate (m)
r_i	external radius of the ceramic tube (m)
r_m	radius of macropores (m)
r_p	radius of micropores (m)
r_0	internal radius of the quartz tube (m)
R_{CO}	rate of CO combustion (mol/m^2/s)
R_w	CH_4 combustion rate (mol/m^3/s)
$Sh_f = K_{g,f} d_h / D_{m,f}$	Sherwood number
u	axial gas velocity (m/s)
z	axial coordinate (m)
Greek letters	
δ_A	size of the annular chamber (m)
δ_w	thickness of catalyst washcoat (m)
ε_m	volume fraction of macropores
ε_p	volume fraction of micropores
ν_f	stoichiometric coefficient of f-species
ρ	gas density (kg/m^3)
Subscripts	
g	gas phase
w	catalyst layer
0	inlet condition

catalytic burners with NO_x emissions below 5 ppm [3] have been launched into the market. Besides several other catalytic combustion devices (premixed radiant burners, industrial boilers, cookers [4,5]) are currently under development.

Industrial applications of catalytic combustion for the production of heat and energy are typically extremely fast and strongly exothermic processes which are operated under very severe conditions [1] with temperatures as high as 800–900°C. Accordingly diffusional limitations and marked temperature gradients can hardly be avoided, which makes laboratory kinetic measurements an arduous task. Furthermore, structured catalysts (monolith honeycombs and foams, fibrous panels) are typically used, whose properties could be significantly different from those of powder or grain catalysts used in conventional laboratory packed bed reactors.

On the other hand structured catalytic reactors can be conceived and designed specifically to obtain chemical kinetics data under extremely severe conditions. Along these lines McCarty [6] developed the annular reactor for investigation of high temperature kinetics of CH_4 combustion on PdO-based catalysts. This structured catalytic reactor consists of a ceramic tube coated with a thin catalyst layer and co-axially placed within a quartz tube to form an annular chamber where the gas flows straightforward. Although no quantitative analysis was reported, McCarty claimed that using small annular gap distances (0.1–0.3 mm) and thin catalyst layers (10–40 μm), CH_4 combustion rate measurements over a palladium-based catalyst were possible at high temperature with minimal thermal and concentration gradients across the gas boundary layer. A similar reactor configuration, but with larger size of the annular chamber and thicker catalyst layer, was adopted by Johansson and Jaras [7] and Beretta et al. [8]. These latter authors also demonstrated that the annular reactor can provide more effective dissipation of reaction heat than conventional laboratory packed bed reactors, likely through radiation from the catalyst skin.

Another structured reactor concept can be exploited to further increase dissipation of reaction heat. By means of mathematical model simulation of a multitubular reactor for highly exothermic processes Groppi and Tronconi [9] theoretically demonstrated the capability of metallic monolith catalysts to secure an extremely efficient dissipation of reaction heat through a proper choice of support material and monolith geometry. This result can be scaled down to laboratory reactors for kinetic measurements by assembling packets of highly conductive metallic slabs coated with thin catalyst layers in a plate-type parallel-passage reactor configuration. Such a concept has been recently demonstrated by experiment [10].

In this paper the potential of both the annular and the metallic plate-type reactors for investigation of catalytic combustion kinetics over very active $PdO/\gamma\text{-}Al_2O_3$ catalysts will be addressed. The design of the annular reactor configuration by modeling analysis, aimed at minimizing diffusional biases, will be illustrated, and kinetic data on high temperature CH_4 catalytic combustion will be presented. Then the heat dissipation properties of the metallic plate-type reactor will be discussed, and kinetic data for combustion of CO at high concentrations will be finally presented.

2. Experimental

2.1. Structured reactors

Figs. 1 and 2 report the schematics of the two investigated structured reactors. In the annular reactor (Fig. 1) the gas flows downwards in the annulus between the ceramic and the quartz tubes. The $PdO/\gamma\text{-}Al_2O_3$ (Pd = 10% (w/w)) catalyst is deposited on the external surface of the ceramic tube, near the bottom of the annular duct to enhance pre-heating of the gas phase. Under the assumption of thermal equilibrium across the transverse section of the ceramic tube, the axial temperature profile of the catalyst is measured by a thermocouple sliding inside the internal cavity of the $\alpha\text{-}Al_2O_3$ tube. In the case of the metallic plate-type reactor (Fig. 2), the catalyst consisted of 12 slabs (width = 46 mm, length = 50 mm),

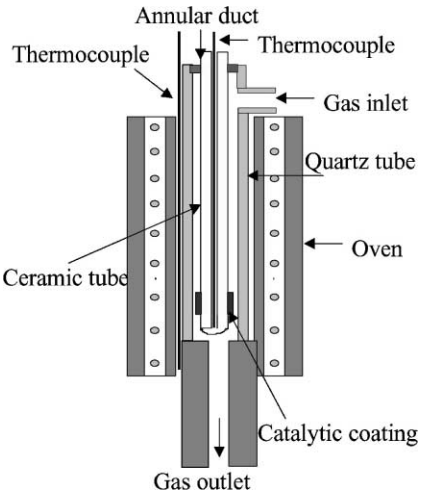

Fig. 1. Schematic diagram of the annular reactor.

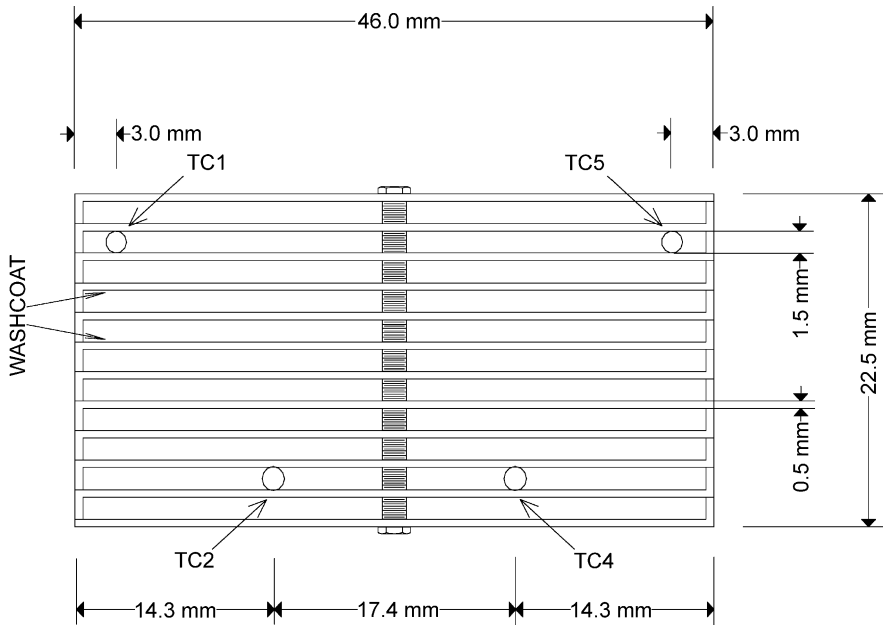

Fig. 2. Schematic diagram of the metallic plate-type reactor.

which were coated with PdO/γ-Al_2O_3 (Pd = 3% (w/w), total coating load = 3.98 g) and assembled with spacers 1.5 mm apart in order to form 11 parallel rectangular channels. The slabs were made of aluminum (99.5% commercial purity) with thickness of 0.5 mm. The plate-type catalyst was eventually equipped with four $\frac{1}{16}$ in. stainless steel tubes at different transverse locations, acting as thermowells for sliding thermocouples, and loaded into a stainless steel reactor tube (46 × 26 mm internal cross-section) placed inside an oven with air recirculation (Mazzali Thermotest), which secured an uniform external temperature distribution. The pressure drop in the reactor was negligible in all runs.

2.2. Catalyst layer

The catalyst layer has been deposited onto both the ceramic tubes and the aluminum slabs via a washcoating procedure partially derived from patent indications [11,12] that is described in details in a companion paper [13]. This technique has allowed to obtain adherent active layers as thin as 5–10 μm which exhibited morphological and catalytic properties close to those of the starting catalytic powders. By N_2 adsorption at 77 K (CarloErba Sorptomatic 1900 series) a surface area of 110 m^2/g was measured. Porosity measurements by Hg penetration provided a pore volume of 0.48 cm^3/g with an average pore radius of 90 Å. Comparison with an active layer density of 0.9 g/cm^3, as derived from weight measurements and thickness evaluation by SEM images, suggest that the actual pore volume has been slightly underestimated, an additional 0.1–0.2 cm^3/g of macropore volume being likely missed by Hg penetration measurements. Finally, CO combustion tests performed in a packed bed filled with catalyst powder and in the structured metallic plate-type reactor provided the same CO_2 productivity at given temperature and CO feed concentration.

2.3. Kinetic tests

The target flow rate and feed composition was obtained with electronic mass flow controllers (Brooks 5850 TR series). Test conditions have been changed depending on the reactor configuration and will be given in details in the following sections. In both CH_4 and CO combustion tests analysis of reactants and products was performed by an online GC (HP 6890 Series) equipped with a Porapak Q and a 5 Å molecular sieve 3 m long packed columns with an in-series TCD detector.

3. Results and discussion

3.1. Design of the annular reactor

3.1.1. Mathematical model

Taking advantage of the well-defined geometry of the annular reactor the design task has been performed by a relatively simple mathematical model derived under the following assumptions: (i) one-dimensional lumped description of the gas phase and two-dimensional distributed description of the catalyst phase; (ii) fully developed laminar flow in the annulus; (iii) steady-state conditions; (iv) isothermal catalyst and gas phase; (v) negligible pressure drop. The model consists of the following mass-balance equations for the gas and catalyst phases which include the contributions of gas–solid external diffusion, axial diffusion in the gas phase, internal diffusion in the catalyst in order to account for all the possible mass transfer biasing on kinetics.

f-Species mass balances ($f = CH_4$, H_2O),

$$u\frac{\partial C_{f,\mathrm{g}}}{\partial z} = \left[(D_{\mathrm{ea},f})\frac{\partial^2 C_{f,\mathrm{g}}}{\partial z^2}\right] - \frac{4}{d_\mathrm{h}}\left[\frac{r_\mathrm{i}+\delta_\mathrm{w}}{r_0+(r_\mathrm{i}+\delta_\mathrm{w})}\right] \times K_{\mathrm{g},f}(C_{f,\mathrm{g}} - C_{f,\mathrm{w}}) \quad \text{gas phase} \tag{1}$$

$$D_{\mathrm{e},f}\frac{\partial^2 C_{f,\mathrm{w}}}{\partial n^2} + \nu_f R_\mathrm{w} = 0 \quad \text{catalyst phase} \tag{2}$$

Boundary conditions,

$$u(C_{f,\mathrm{g}} - C^0_{f,\mathrm{g}}) = D_{\mathrm{m},f}\frac{\partial C_{f,\mathrm{g}}}{\partial z} \quad \text{at } z = 0 \tag{3}$$

$$\frac{\partial C_{f,\mathrm{g}}}{\partial z} = 0 \quad \text{at } z = L \tag{4}$$

$$D_{\mathrm{e},f}\frac{\partial C_{f,\mathrm{w}}}{\partial n} = K_{\mathrm{g},f}(C_{f,\mathrm{g}} - C_{f,\mathrm{w}}) \quad \text{at g/w interface, } n = \delta_\mathrm{w} \tag{5}$$

$$\frac{\partial C_{f,\mathrm{w}}}{\partial n} = 0 \quad \text{at catalyst/}\alpha\text{-}Al_2O_3\text{ interface, } n = 0 \tag{6}$$

The PDEs (1)–(6) have been solved numerically in dimensionless form [14].

The design of the annular reactor has been performed by simulating CH_4 lean combustion tests over a very active PdO-based catalyst under conditions which typically correspond to very fast reactions. Pressure has been set to 1 bar in line with the assumption of negligible pressure drop. The following kinetic expression has been adopted for methane combustion over Pd-based catalysts which include H_2O inhibition reported in the literature [15,16]:

$$R_w = \left(\frac{K_r C_{CH_4,w}}{1 + K_{H_2O} C_{H_2O,w}} \right) \ (\text{mol}/(\text{m}^3\,\text{s})) \qquad (7)$$

Kinetic parameters have been fixed so as to simulate a very fast reaction providing 60% conversion at 600°C, GHSV $= 3 \times 10^6\,\text{h}^{-1}$, with a water free feed. Two types of catalyst morphology have been considered: one monomodal pore size distribution, that has been directly derived from the experimental values, and one bimodal pore size distribution with a significant macropore fraction which, as mentioned above, can be inferred from considerations on the active layer density. Sherwood numbers for calculation of external mass transfer coefficients have been derived from the heat transfer literature [17] on the basis of the analogy with the Graetz thermal problem ($Sh = 5.385$). The set of model parameters used in the reactor design analysis are summarized in Table 1.

In the simulations the radius of the quartz tube and the length of the catalyst bed have been fixed, whereas the size of the annular chamber and the thickness of the catalyst layer have been varied as design parameters of the reactor geometry.

3.2. Simulation results

The following global reactor effectiveness factor has been defined as design target:

$$\eta_{glob} = \frac{K_r^{eff}}{K_r} \qquad (8)$$

This represents the ratio to the actual kinetic constant, K_r, of the value K_r^{eff} that must be included in a simple plug-flow, pseudo-homogeneous mathematical model of the annular reactor to calculate the same CH_4 conversion provided by the more complex model described above. Accordingly η_{glob} corresponds to the relative error on the estimates of the rate constant associated with the analysis of conversion data when neglecting any diffusional phenomena.

Simulation results for the monomodal pore size distributions, reported in Fig. 3, show that the calculated global efficiency rapidly decreases on

Table 1
Simulation parameters for the annular reactor

Kinetics		
$K_r = 3.992 \times 10^3\ (s^{-1})$		
$K_{H_2O}\ (m^3/mol) = 3.509$		
Catalyst morphology		
Pore distribution	$D_{e,f}^{CH_4}\ (m^2/s)$	$D_{e,f}^{H_2O}\ (m^2/s)$
Monomodal		
$\varepsilon_p = 0.5225, r_p = 9\,nm$	1.102×10^{-6}	1.042×10^{-6}
Bimodal		
$\varepsilon_p = 0.5225, r_p = 9\,nm$	3.060×10^{-6}	2.909×10^{-6}
$\varepsilon_m = 0.1, r_m = 100\,nm$		
Gas properties		
$C_{tot}\ (mol/m^3)$	13.97	
$D_{m,f}\ (m^2/s)$	$3.379 \times 10^{-4}\ (CH_4)$	$3.826 \times 10^{-4}\ (H_2O)$
Operating conditions		
Flow rate = 1.67 (cm^3/s at STP), $T = 873$ (K), $P = 1$ (bar)		
Feed composition (v/v): 20% O_2; 0.75% CH_4; He to balance		
Geometry		
$L = 1.0 \times 10^{-2}$ (m), $r_0 = 3.50 \times 10^{-3}$ (m)		

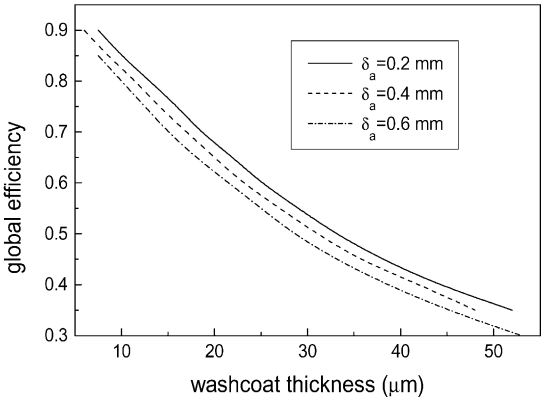

Fig. 3. Effect of catalyst layer thickness and annular chamber height on the calculated global efficiency of the annular reactor (monomodal pore distribution).

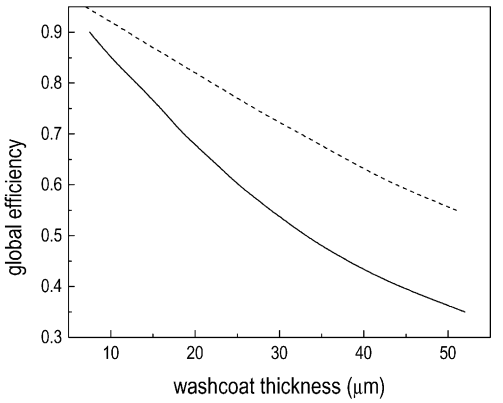

Fig. 4. Comparison of calculated global annular reactor efficiencies with monomodal pore distribution (solid line) and with bimodal pore distribution (dotted line). $\delta_A = 0.2$ mm.

increasing the catalyst washcoat thickness δ_w. Due to the very fast combustion kinetics assumed in the simulations, global efficiencies below 0.5 are obtained for active layers thicker than 30–35 μm. In view of this the catalyst thickness must be kept as low as 10 μm to achieve global efficiencies close to 0.9. On the other hand the size of the annular chamber shows a minor impact, the global efficiency decreasing only by 5% on increasing δ_A by a factor of 3. These results point out that, with a reasonably small annular chamber, internal diffusion within the catalyst pores is by far the most critical phenomenon which biases kinetic measurements. The residual effect of δ_A is associated with both the gas–solid external diffusion and the axial diffusion in the gas phase, the contribution of the latter being the most important one as demonstrated by diagnostic simulations performed by setting $D_{ea,f} = 0$.

The key role of internal diffusion is further demonstrated in Fig. 4, where simulation results obtained with the monomodal and the bimodal pore size distributions are compared. The enhanced diffusion rate associated with the presence of a significant macropore fraction (see Table 1) results in a marked improvement of the calculated global efficiency.

On the basis of the results above a reactor design with $\delta_w = 10$ μm and $\delta_A = 0.25$ mm has been derived to minimize the impact of diffusional phenomena so as to achieve a global efficiency close to 0.9. It is worth mentioning that the calculated 10% error associated with neglecting diffusion bias in such a reactor configuration is of the same order of the experimental error associated with conversion measurements with a ±5% relative accuracy.

3.2.1. Experimental performances of the annular reactor

The design configuration above has been realized by assembling a 6.5 mm OD α-Al_2O_3 tube, properly coated with a catalytic active layer, with a 7.0 mm ID quartz tube. The experimental performances of this reactor have been preliminary tested in order to check the potentialities to collect kinetic data under high-*T*–high GHSV conditions. The following major results have been obtained:

1. Pressure drops are practically negligible (below 0.1 bar) at a flow rate of 100 cm^3/min at STP which corresponds to a GHSV $= 3 \times 10^6$ $cm^3/(g\,h)$: such a flow rate has been adopted in all the subsequent tests.
2. Blank experiments indicate that the role of homogeneous combustion is negligible up to 850°C and still small at 900°C (CH_4 conversion below 10%). Such a minimal role of homogeneous reactions can be partly related to a wall quenching effect associated with the very small size of the annular chamber.
3. In preliminary combustion tests, partial CH_4 conversion (<65%) has been obtained up to 600°C proving the possibility to obtain kinetic data at high temperature (under typical test conditions with a

conventional laboratory packed bed reactor complete conversion was achieved already at 450°C).

4. The same conversion values have been obtained using either He or N_2 as carrier gases confirming the negligible role of external gas–solid and axial gas phase diffusion.
5. Overall temperature differences along the catalyst have been kept below 10°C with CH_4 inlet concentration up to 3% and conversion values up to 70%. Further CO and CH_4 combustion and blank tests performed in the 250–600°C range and measuring axial temperature in the internal cavity of the ceramic tube, on the external wall of the quartz tube and on the furnace wall have confirmed that radiation is the most effective mechanism of reaction heat dissipation at high temperature. However also convection plays some role due to the very small size of the annular chamber.

3.2.2. CH_4 combustion kinetics

On the basis of the above results an extended kinetic study of CH_4 combustion over the PdO/γ-Al_2O_3 catalyst with high metal loading has been then attempted in the following variable range: T = 400–600°C; H_2O_{in} = 0–9% (v/v), $CH_{4\,in}$ = 0.8–3% (v/v), $O_{2\,in}$ = 5–20% (v/v), He to balance; GHSV = $3 \times 10^6\,cm^3/(g\,h)$. Although deactivation problems prevent to obtain well-defined kinetics, several indications have been collected on high temperature reaction rates which are reported in details in [18]. As one of the most prominent results, data have been obtained on the effect of water in the high temperature range. Indeed water inhibition had been previously reported in the literature [15,16] on the basis of kinetic data collected up to 400°C but no direct evidence was available above this temperature. Table 2 summarizes conversion data obtained in this work at different temperatures and H_2O concentrations in the feed. The data clearly show that H_2O strongly inhibits the reaction in all the investigated temperature range. As documented by the parity plot in Fig. 5 the effects of H_2O concentration along with those of O_2 and CH_4 concentration have been nicely fitted using the following rate expression, similar to that adopted in the design analysis, with parameters reported in Table 3.

Table 2
Experimental conversion data at different temperature and feed % H_2O (feed composition: 0.8% CH_4, 20% O_2, x% H_2O, He to balance)

T (°C)	Feed % H_2O				
	0%	1%	3%	6%	9%
450	20.8	10.4	<5	<5	<5
500	35.2	21.8	15.4	<5	<5
550	49.8	35.8	28.0	15.5	10.6
600	64.4	50.3	42.5	28.7	23.9

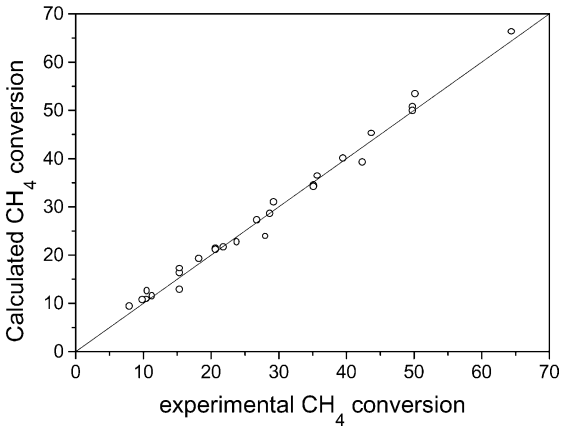

Fig. 5. Parity plot for the kinetic analysis of CH_4 combustion in the annular reactor.

$$R_w = \frac{K_r C_{CH_4}}{1 + K_{H_2O} C_{H_2O}}\ (\mathrm{mol/(kg\,s)}) \tag{9}$$

3.2.3. CO oxidation in the plate-type metallic reactor

In the following section we address the application of a second structured system, namely the "high conductivity" plate-type reactor, to the kinetic study of catalytic combustion reactions.

Previous theoretical [9,19] and experimental [10] investigations on the factors affecting removal of the reaction heat in structured catalysts with conductive supports have shown that the thermal behavior of

Table 3
Estimated values of kinetic parameters in the rate expression for CH_4 combustion over the 10% PdO/γ-Al_2O_3 catalyst, Eq. (9)

K_r at 773 K = $1.2\,m^3/kg/s$
E_{att} = 63.6 kJ/mol
K_{H_2O} at 773 K = $5.00\,m^3/mol$
$\Delta H_{H_2O} = -20.8$ kJ/mol

such systems is influenced primarily by the intrinsic thermal conductivity of the support material and by the geometrical features of the support. Particularly, plate-type catalysts with highly conductive metallic slabs would significantly decrease the hot spot temperatures as compared to catalysts with thinner slabs made of less conductive metals. Thermal contact between the assembled slab packet and the inner wall of the reactor tube was also identified as one of the most critical factors which affect the overall efficiency of heat dissipation [10].

In line with such indications, the design of the plate-type catalyst/reactor system for the present work was based on Al slabs with 0.25 mm half-thickness and with additional appendixes at the end of each slab, which provide an increased contact area with the internal reactor wall, in order to achieve an excellent heat removal efficiency so as to cover a broader range of conditions when investigating the kinetics of strongly exothermic catalytic reactions. To prove this concept an extensive set of CO oxidation runs was performed in the metallic plate-type reactor: in such runs, the reactor feed stream consisted of 0.7–8.8% (v/v) CO in air or air/N_2 (O_2 concentration = 4–19% (v/v)), with feed flow rates in the range 1000–9000 cm^3/min (STP) (GHSV = 16 000–150 000 $cm^3/(g\,h)$), always corresponding to laminar flow conditions in the catalyst channels. The catalyst temperature was varied between 105 and 450°C.

A first series of CO combustion runs in air was specifically devoted to investigating the thermal behavior of the metallic plate-type reactor. Fig. 6 shows temperature distributions measured in the reactor at 5% CO feed content and with high feed flow rates. At the considered oven temperature of 196°C total CO conversion was always achieved corresponding to considerably high thermal loads (dissipated heat power up to ∼100 W). As a result the temperature of the metallic slabs was markedly higher than the oven temperature, the difference increasing consistently with the flow rate. Nonetheless the temperature profile throughout the structured catalyst was essentially uniform thanks to the capability of the metallic slabs to distribute the reaction heat. At less severe conditions, i.e. either lower flow rate and CO inlet concentration or partial CO conversion, the reactor was essentially isothermal. Thus the efficiency exhibited by the metallic plate-type reactor in distributing and removing the heat of CO combustion prompted us to investigate further its potential with respect to the kinetic study of highly exothermic catalytic reactions, including catalytic combustion reactions as well as, e.g. partial oxidations of hydrocarbons.

Fig. 7 shows CO conversion data measured in CO oxidation with air for different CO feed contents at a fixed feed flow rate. The marked conversion delay with increasing feed concentration of CO corresponds to a negative reaction order with respect to CO, in line with previous reports on the kinetics of CO oxidation over noble metal catalysts [20,21]. Conversion data in Fig. 7 along with the results of other experiments addressing the effect of O_2 and CO_2 concentration have been fitted with the empirical form of the rate expression, Eq. (10), based on literature kinetic studies

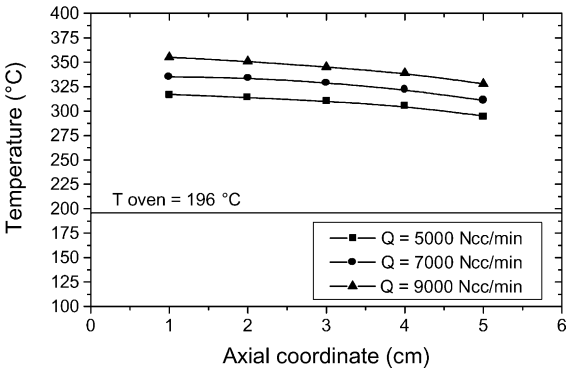

Fig. 6. Measured temperature profiles in CO combustion runs in the plate-type metallic reactor at different flow rates. Feed composition: $Y^0_{CO} = 0.05$ in air.

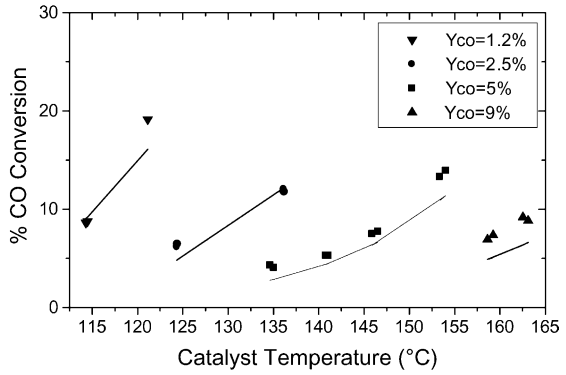

Fig. 7. Effect of CO inlet concentration on CO conversion. Symbols: experimental data; lines: values predicted with Eq. (10). Feed flow rate $Q = 1800\,N\,cm^3$/min.

Table 4
Estimated values of kinetic parameters in the rate expression for CO combustion over the 3% PdO/γ-Al_2O_3 catalyst, Eq. (10)

k_1 at 473 K = 27.4 mol/kg/s/$bar^{3/2}$
E_{att} = 17.2 kJ/mol
K_{CO} at 473 K = 84.8 bar^{-1}
ΔH_{CO} = −39.9 kJ/mol

of CO oxidation over noble metal catalysts [20–22]:

$$R_{CO} = \frac{k_1 p_{CO} p_{O_2}^{1/2}}{(1 + K_{CO} p_{CO})^2} \ (\text{mol}/(\text{kg s})) \qquad (10)$$

Table 4 provides the estimates of the four rate parameters. As an example of the model fit, predicted values of CO conversion are reported in Fig. 7. Despite of some residual discrepancies it is evident that the effect of the CO concentration in the feed is reasonably accounted for in a much broader range than those included in previous literature kinetic studies.

Rate equation (10) was successfully applied to the kinetic analysis of CO oxidation over other structured catalysts samples with Pd/Al_2O_3 washcoats. It was also included in a nonisothermal model of the metallic plate-type reactor, by which an engineering analysis of the thermal behavior of such a reactor was carried out [10].

4. Conclusions

The experimental and theoretical results presented in this paper have demonstrated specifically designed structured catalytic reactors as effective tools for kinetic investigation of catalytic combustion reactions under severe conditions.

The following major advantages have been pointed out:

1. The parallel flow pattern guarantees negligible pressure drop with high flow rates, so that tests with extremely high GHSV can be performed to investigate kinetics of ultra-fast reactions under conditions representative of their industrial application.
2. The regular geometry allows to define accurately the fluid dynamics and particularly the gas/solid contact, even in the case of catalyst loads of a few milligrams which are hardly handled in conventional packed bed reactors; this can be exploited for reliable reactor design and analysis by mathematical modeling.
3. The impact of diffusional processes can be minimized via reactor design combined with appropriate coating techniques.
4. An effective dissipation of reaction heat can be achieved through different mechanisms (radiation, convection and conduction), which are typically not available in conventional packed bed reactors.
5. The procedures followed for the preparation of the investigated structured catalysts, which are obtained by deposition of active catalytic layers onto ceramic or metallic supports, closely resemble those adopted for production of industrial monolith catalysts, which guarantees the practical significance of the kinetic data.

The annular reactor configuration provides a good example of how such advantages are combined into a device that can be manufactured in a very small scale with conventional laboratory techniques and materials. In those cases where dissipation of the reaction heat becomes the paramount issue, the plate-type metallic reactor can represent a valuable solution.

Acknowledgements

Financial support for this work was provided by MURST, Rome, Italy and by Japan Cooperation Center Petroleum, Tokyo, Japan.

References

[1] G. Groppi, P. Forzatti, Catal. Today 54 (1999) 165.
[2] Published on the web site www.catalyticaenergy.com.
[3] S. Ro, A. Scholten, Catal. Today 47 (1999) 415.
[4] I. Cerri, G. Saracco, F. Geobaldo, V. Specchia, Ind. Eng. Chem. Res. 39 (2000) 24.
[5] A. Scholten, R. Van Yperen, J. Emmerzaal, in: Proceedings of the Fourth IWCC, Book of Abstract, San Diego, CA, April 14–16, 1999, p. 35.
[6] J. McCarty, Catal. Today 26 (1995) 283.
[7] E.M. Johansson, S.G. Jaras, Catal. Today 47 (1999) 359.
[8] A. Beretta, P. Baiardi, D. Prina, P. Forzatti, Chem. Eng. Sci. 54 (1999) 765.

[9] G. Groppi, E. Tronconi, Chem. Eng. Sci. 55 (2000) 2161.
[10] E. Tronconi, G. Groppi, Chem. Eng. Sci. 55 (2000) 6021.
[11] S. Yasaki, Y. Yoshino, K. Ihara, K. Ohkubo, US Patent 5 208 206 (1993).
[12] R.A. Dalla Betta, T. Shoij, K. Tsurumi, N. Ezawa, US Patent 5 250 489 (1993).
[13] M. Valentini, G. Groppi, C. Cristiani, M. Levi, E. Tronconi, P. Forzatti, Catal. Today 69 (2001) 307.
[14] B. Finlayson, Nonlinear Analysis in Chemical Engineering, McGraw-Hill, New York, 1980.
[15] K. Fujimoto, F.H. Ribeiro, M. Avalos-Borja, E. Iglesia, J. Catal. 179 (1999) 431.
[16] J.C. Van Giezen, F.N. Van Den Berg, J.L. Kleinen, A.J. Van Dillen, J.W. Geus, Catal. Today 47 (1999) 287.
[17] R.K. Shah, A.L. London, Laminar Flow Forced Convection, Academic Press, New York, 1978.
[18] G. Groppi, W. Ibashi, M. Valentini, P. Forzatti, Chem. Eng. Sci. 56 (2001) 831.
[19] G. Groppi, E. Tronconi, AIChE J. 42 (1996) 2382.
[20] S.E. Voltz, C.R. Morgan, B.A. Liederman, Ind. Eng. Chem. Process. Des. Dev. 12 (1973) 294.
[21] B. Subramanian, A. Varma, Ind. Eng. Chem. Process. Des. Dev. 24 (1985) 512.
[22] C. Dubien, D. Schweich, G. Mabilon, B. Martin, M. Prigent, Chem. Eng. Sci. 53 (1998) 471.